

# COLD-FLUID EQUILIBRIUM OF A LARGE-ASPECT-RATIO ELLIPSE-SHAPED CHARGED-PARTICLE BEAM IN A NON-AXISYMMETRIC PERIODIC PERMANENT MAGNET FOCUSING FIELD\*

Jing Zhou<sup>#</sup>, Ronak Bhatt, and Chiping Chen

Plasma Science and Fusion Center, MIT, Cambridge, MA 02139, U.S.A.

## Abstract

A new class of equilibrium is discovered for a large-aspect-ratio ellipse-shaped charged-particle beam in a non-axisymmetric periodic permanent magnet focusing field. A paraxial cold-fluid model is employed to derive the equilibrium flow properties and generalized envelope equations with negligibly small emittance. A periodic beam equilibrium solution is obtained numerically from the generalized envelope equations. It is shown that the beam edges are well confined in both transverse directions, and that the equilibrium beam exhibits a periodic small-amplitude twist as it propagates. A two-dimensional particle-in-cell (PIC) code, PFB2D, is used to verify the theoretical predictions in the paraxial limit, and to establish validity under non-paraxial situations.

High-intensity ribbon (thin sheet) beams are of great interest in the design and operation of particle accelerators, such as storage rings and rf and induction linacs, as well as vacuum electron devices, such as klystrons and traveling-wave tubes with periodic permanent magnet (PPM) focusing [1-7], because of the following remarkable properties. First, they can transport large amounts of beam currents at reduced intrinsic space-charge forces and energies. Second, they couple efficiently to rectangular rf structures. The combination of the space charge reduction and efficient coupling allows efficient rf generation in vacuum electronic devices, and efficient acceleration in particle accelerators. Third, elliptic beams provide an additional adjustable parameter (e.g., the aspect ratio) which may be useful for better matching a beam into a periodic focusing channel.

We present an equilibrium theory of an elliptic cross-section space-charge-dominated beam in a non-axisymmetric periodic magnetic focusing field. A paraxial cold-fluid model is employed to derive generalized envelope equations which determine the equilibrium flow properties of ellipse-shaped beams with negligibly small emittance. A matched envelope solution is obtained numerically from the generalized envelope equations, and the results show that the beam edges in both transverse directions are well confined, and that the angle of the beam ellipse exhibits a periodic small-amplitude twist. Two-dimensional (2D) particle-in-cell (PIC) simulations with our Periodic Focused Beam 2D (PFB2D) code show good agreement with the predictions of equilibrium theory as well as beam stability.

\*Work supported by the U.S. DOE, office of HEP, DE-FG02-95ER40919, Office of FES, DE-FG02-01ER54662, Air Force Office of Scientific Research, F49620-03-1-0230, and the MIT Deshpande Center for Technological Innovation.

<sup>#</sup>jea\_zhou@mit.edu

We consider a high-intensity, space-charge-dominated beam, in which kinetic (emittance) effects are negligibly small. The beam can be adequately described by cold-fluid equations. In the paraxial approximation, the steady-state cold-fluid equations for time-stationary flow ( $\partial/\partial t = 0$ ) in cgs units are [8, 9]

$$\beta_b c \partial n_b / \partial s + \nabla_{\perp} \cdot (n_b \mathbf{V}_{\perp}) = 0, \quad (1)$$

$$\nabla_{\perp}^2 \phi^s = \beta_b^{-1} \nabla_{\perp}^2 A_z^s = -4\pi q n_b, \quad (2)$$

$$n_b \left( \beta_b c \frac{\partial}{\partial s} + \mathbf{V}_{\perp} \cdot \nabla_{\perp} \right) \mathbf{V}_{\perp} = \frac{q n_b}{\gamma_b m} \left[ -\frac{1}{\gamma_b^2} \nabla_{\perp} \phi^s + \beta_b \hat{\mathbf{e}}_z \times \mathbf{B}_{\perp}^{ext} + \frac{\mathbf{V}_{\perp}}{c} \times B_z^{ext}(s) \hat{\mathbf{e}}_z \right], \quad (3)$$

where  $s = z$ ,  $\mathbf{x}_{\perp} = x \hat{\mathbf{e}}_x + y \hat{\mathbf{e}}_y$ ,  $\nabla_{\perp} = \partial/\partial \mathbf{x}_{\perp}$ ,  $q$  and  $m$  are the particle charge and rest mass, respectively,  $n_b$  is the particle density,  $\mathbf{V}_{\perp}$  is the transverse flow velocity,  $\gamma_b = (1 - \beta_b^2)^{-1/2}$  is the relativistic mass factor, use has been made of  $\beta_z = V_z/c \cong \beta_b = const$ ,  $c$  is the speed of light in vacuum, and the self-electric field  $\mathbf{E}^s$  and self-magnetic field  $\mathbf{B}^s$  are determined from the scalar potential  $\phi^s$  and vector potential  $A_z^s \hat{\mathbf{e}}_z$ , i.e.,  $\mathbf{E}^s = -\nabla_{\perp} \phi^s$  and  $\mathbf{B}^s = \nabla_{\perp} \times A_z^s \hat{\mathbf{e}}_z$ .

For the beam dimensions small relative to the characteristic scale of magnetic variations, i.e.,  $(k_{0x} x)^2/6 \ll 1$  and  $(k_{0y} y)^2/6 \ll 1$ , a three-dimensional (3D) non-axisymmetric periodic magnetic field can be described to the lowest order in the transverse dimension as [9]

$$\mathbf{B}^{ext}(\mathbf{x}) \cong B_0 \left[ \frac{k_{0x}^2}{k_0} \cos(k_0 s) x \hat{\mathbf{e}}_x + \frac{k_{0y}^2}{k_0} \cos(k_0 s) y \hat{\mathbf{e}}_y - \sin(k_0 s) \hat{\mathbf{e}}_z \right], \quad (4)$$

where  $k_0 = 2\pi/S$ ,  $k_{0x}^2 + k_{0y}^2 = k_0^2$ , and  $S$  is the axial periodicity length. The 3D magnetic field in Eq. (4) is fully specified by the three parameters  $B_0$ ,  $S$  and  $k_{0x}/k_{0y}$ .

We seek solutions to Eqs. (1)-(3) of the form [9]

$$n_b(\mathbf{x}_{\perp}, s) = \frac{N_b}{\pi a(s) b(s)} \Theta \left[ 1 - \frac{\tilde{x}^2}{a^2(s)} - \frac{\tilde{y}^2}{b^2(s)} \right], \quad (5)$$

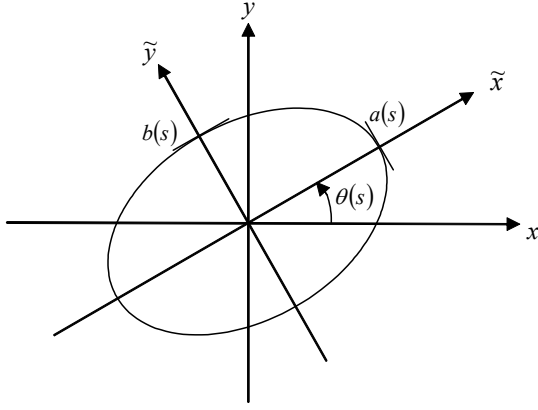


Figure 1: Laboratory and twisted coordinate systems.

$$\mathbf{V}_\perp(\mathbf{x}_\perp, s) = [\mu_x(s)\tilde{x} - \alpha_x(s)\tilde{y}]\beta_b c\hat{\mathbf{e}}_{\tilde{x}} + [\mu_y(s)\tilde{y} + \alpha_y(s)\tilde{x}]\beta_b c\hat{\mathbf{e}}_{\tilde{y}}. \quad (6)$$

In Eqs. (5) and (6),  $\mathbf{x}_\perp = \tilde{x}\hat{\mathbf{e}}_{\tilde{x}} + \tilde{y}\hat{\mathbf{e}}_{\tilde{y}}$  is a transverse displacement in the twisted coordinate system illustrated in Fig. 1;  $\theta(s)$  is the twist angle of the ellipse;  $\Theta(x) = 1$  if  $x > 0$  and  $\Theta(x) = 0$  if  $x < 0$ ; and the functions  $a(s)$ ,  $b(s)$ ,  $\mu_x(s)$ ,  $\mu_y(s)$ ,  $\alpha_x(s)$ ,  $\alpha_y(s)$  and  $\theta(s)$  are to be determined self-consistently [see Eqs. (8)-(12)].

The self-electric and self-magnetic fields are well known for an elliptical beam with density distribution specified in Eq. (5), i.e.,

$$\phi^s = \beta_b^{-1} A_z^s = -\frac{2qN_b}{a+b} \left( \frac{\tilde{x}^2}{a} + \frac{\tilde{y}^2}{b} \right). \quad (7)$$

Using the expressions in Eqs. (4)-(7) and following the technique in [8, 9], it can be shown that both the equilibrium continuity equation (1) and force equation (3) are satisfied if the dynamical variables  $a(s)$ ,  $b(s)$ ,  $\mu_x(s) \equiv a^{-1} da/ds$ ,  $\mu_y(s) \equiv b^{-1} db/ds$ ,  $\alpha_x(s)$ ,  $\alpha_y(s)$  and  $\theta(s)$  obey the generalized beam envelope equations [9]

$$\frac{d^2 a}{ds^2} - \left[ \frac{b^2(\alpha_x^2 - 2\alpha_x\alpha_y) + a^2\alpha_y^2}{a^2 - b^2} - 2\sqrt{\kappa_{z0}}\alpha_y \sin(k_0 s) + \sqrt{\kappa_{z0}} \frac{k_{0x}^2 - k_{0y}^2}{k_0} \cos(k_0 s) \sin(2\theta) \right] a - \frac{2K}{a+b} = 0, \quad (8)$$

$$\frac{d^2 b}{ds^2} + \left[ \frac{a^2(\alpha_y^2 - 2\alpha_x\alpha_y) + b^2\alpha_x^2}{a^2 - b^2} + 2\sqrt{\kappa_{z0}}\alpha_x \sin(k_0 s) + \sqrt{\kappa_{z0}} \frac{k_{0x}^2 - k_{0y}^2}{k_0} \cos(k_0 s) \sin(2\theta) \right] b - \frac{2K}{a+b} = 0, \quad (9)$$

$$\frac{d}{ds} (a^2 \alpha_y) - 2\sqrt{\kappa_{z0}} \cos(k_0 s) \frac{k_{0x}^2 \cos^2 \theta + k_{0y}^2 \sin^2 \theta}{k_0} a^2$$

$$- \frac{ab^3(\alpha_x - \alpha_y)}{a^2 - b^2} \frac{d}{ds} \left( \frac{a}{b} \right) - 2\sqrt{\kappa_{z0}} a \frac{da}{ds} \sin(k_0 s) = 0, \quad (10)$$

$$\frac{d}{ds} (b^2 \alpha_x) - 2\sqrt{\kappa_{z0}} \cos(k_0 s) \frac{k_{0x}^2 \sin^2 \theta + k_{0y}^2 \cos^2 \theta}{k_0} b^2$$

$$- \frac{a^3 b(\alpha_x - \alpha_y)}{a^2 - b^2} \frac{d}{ds} \left( \frac{b}{a} \right) - 2\sqrt{\kappa_{z0}} b \frac{db}{ds} \sin(k_0 s) = 0, \quad (11)$$

$$\frac{d\theta}{ds} = \frac{a^2 \alpha_y - b^2 \alpha_x}{a^2 - b^2}, \quad (12)$$

where  $\sqrt{\kappa_{z0}} \equiv qB_0/2\gamma_b\beta_b mc^2$  and  $K \equiv 2qI_b/\gamma_b^3\beta_b^3 mc^3$ .

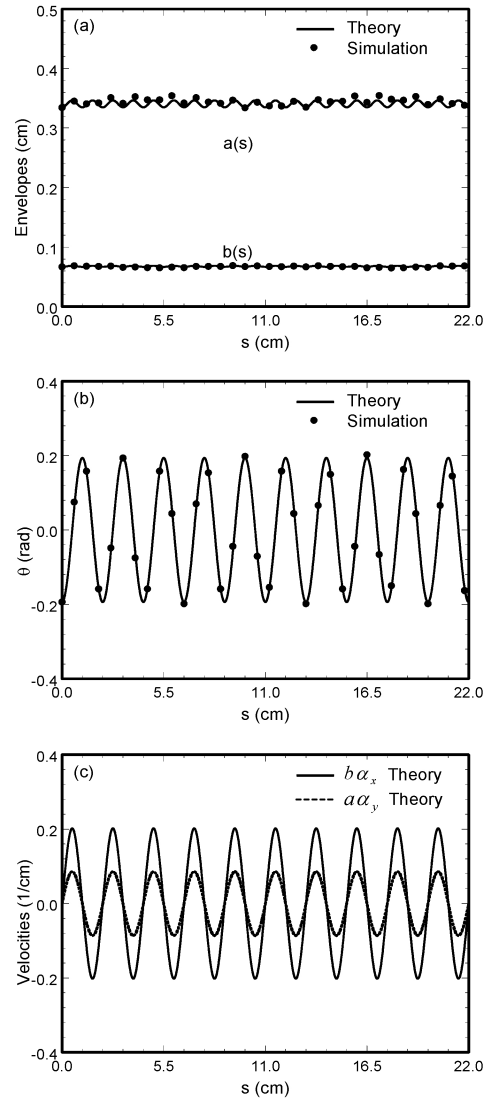


Figure 2: Plots of (a) envelopes  $a(s)$  and  $b(s)$ , (b) twist angle  $\theta(s)$ , and (c) normalized rotational velocities  $b(s)\alpha_x(s)$  and  $a(s)\alpha_y(s)$  versus the axial distance  $s$  for the relativistic beam in Table 1. The solid and dashed curves are the generalized envelope solution, whereas the dotted curves are from the PFB2D simulation.

Equations (8)-(12) have “time” reversal symmetry under the transformation  $(s, a, b, a', b', \alpha_x, \alpha_y, \theta) \rightarrow (-s, a, b, -a', -b', -\alpha_x, -\alpha_y, \theta)$ . This implies that the dynamical system described by Eqs. (8)-(12) has the hyper symmetry plane  $(a', b', \alpha_x, \alpha_y)$ .

A numerical module in the PFB2D code has been developed to solve the generalized envelope equations (8)-(12). There are, in total, seven functions  $a(s)$ ,  $b(s)$ ,  $a'(s)$ ,  $b'(s)$ ,  $\alpha_x(s)$ ,  $\alpha_y(s)$  and  $\theta(s)$  to be determined. The time inverse symmetry of the dynamical system requires the quantities  $(a', b', \alpha_x, \alpha_y)$  vanish at  $s=0$  for matched solutions, therefore, only the three initial values  $a(0)$ ,  $b(0)$  and  $\theta(0)$  corresponding to a matched solution need to be determined with Newton’s method. The beam equilibria predicted by the generalized envelope equations are verified by 2D PIC simulations using the PFB2D code over a wide range of system parameters. In the PFB2D simulations, we use the paraxial field in Eq. (4), typically  $5 \times 10^5$  particles, a square grid with  $400 \times 400$  cells, and a square conducting pipe with a full width which is 3 times the semi major axis of the beam.

As an example, we consider a relativistic ribbon beam with voltage  $V_b = 114$  keV, current  $I_b = 32.75$  A, aspect ratio  $a/b = 5$ , and non-axisymmetric periodic permanent magnet focusing with  $B_0 = 2.2$  kG,  $S = 2.2$  cm, and  $k_{0y}/k_{0x} = 1.52$  (see Table 1). [We propose four such beams in a 10 MW L-Band multiple-ribbon-beam klystron (MRBK) for a linear collider (LC).] For such a system the matched solution of the generalized envelope equations (8)-(12) is calculated numerically as shown in Figs. 2(a)-2(c) with the corresponding parameters:  $k_{0x} = 1.56$  cm<sup>-1</sup>,  $k_{0y} = 2.39$  cm<sup>-1</sup>,  $\sqrt{\kappa_{z0}} = 0.917$  cm<sup>-1</sup>, and  $K = 1.11 \times 10^{-2}$ . The solution to the generalized envelope equations (8)-(12) shows that the semi-axes of the elliptical beam remain roughly constant with small oscillations, that the orientation of the ellipse twists periodically with an amplitude of ten degrees, and that the normalized rotation flow velocities  $\alpha_x$  and  $\alpha_y$  oscillate with the magnet periodicity. Shown in Figs. 2(a) and 2(b), the dotted curves are the envelopes and angle of the beam ellipse obtained from the PFB2D simulation. It is worthwhile pointing out that the normalized velocities  $\mu_x$ ,  $\mu_y$ ,  $\alpha_x$  and  $\alpha_y$  vanish at  $s=0$  which makes it a natural matching point for a parallel-flow beam with negligibly small emittance [10].

Although high-intensity twisted ribbon-beam equilibria exist over a wide region of parameters ranging from the nonrelativistic to relativistic regimes. In addition to the relativistic ribbon-beam equilibrium discussed above, we present a nonrelativistic ribbon-beam equilibrium and a mildly relativistic ribbon-beam equilibrium in Table 1. The nonrelativistic ribbon beam corresponds to a beam design for a high-efficiency 200 W ribbon-beam amplifier

Table 1: System parameters for ribbon-beam examples

| Parameters        | Nonrelativistic | Mildly Relativistic | Relativistic |
|-------------------|-----------------|---------------------|--------------|
| Current (A)       | 0.11            | 18.5                | 32.75        |
| Voltage (kV)      | 2.29            | 45.0                | 114          |
| $S$ (cm)          | 1.912           | 2.626               | 2.2          |
| $k_{0y} / k_{0x}$ | 1.60            | 1.44                | 1.52         |
| $B_0$ (kG)        | 0.337           | 1.099               | 2.20         |
| $a / b$           | 6.0             | 4.0                 | 5.0          |
| $a$ cm            | 0.373           | 0.585               | 0.335        |
| $\theta_{\max}$   | 10.4°           | 11.5°               | 11.1°        |

(RBA) which is being developed at Massachusetts Institute of Technology (MIT) for communication, whereas the mildly relativistic ribbon beam is proposed for a high-power, high-efficiency RBA for radar applications. Both examples have also been verified by the PFB2D simulations. The results are qualitatively the same as the relativistic example shown in Fig. 2.

In conclusion, a novel exact paraxial cold-fluid equilibrium was found for a high-intensity, space-charge-dominated charged-particle beam with a periodically twisted elliptical cross section in a non-axisymmetric periodic magnetic field. Generalized envelope equations, which determine the beam envelopes, ellipse orientation, density, and internal flow velocity profiles, were derived, and solved numerically for nonrelativistic and relativistic examples of such beams. The equilibrium and stability of such beams were demonstrated by self-consistent particle-in-cell (PIC) simulations. We anticipate that the equilibrium theory will provide a valuable tool in the design of high-intensity ribbon beams in novel vacuum electronic devices, especially for ribbon-beam klystrons and traveling-wave tubes. The ellipse-shaped beam equilibrium may provide some flexibility in the design and operation of high-intensity accelerators.

## REFERENCES

- [1] P. A. Sturrock, *J. Electron. Control* **7**, 162 (1959).
- [2] Z. X. Zhang, V. L. Granatstein, W.W. Destler, *et al.*, *IEEE Tran. Plasma Sci.* **21**, 760 (1993).
- [3] J. H. Booske, B. D. McVey, and T. M. Antonsen, Jr., *J. Appl. Phys.* **73**, 4140 (1993).
- [4] J. H. Booske, A. H. Kumbasar, and M. A. Basten, *Phys. Rev. Lett.* **71**, 3979 (1993).
- [5] M. A. Basten and J. H. Booske, *J. Appl. Phys.* **85**, 6313 (1999).
- [6] B.E. Carlsten, S. J. Russell, L. M. Earley, *et al.*, *31<sup>st</sup> Int. Conf. Plasma Sci. (ICOPS)*, 2004, p. 422.
- [7] G. Caryotakis *et al.*, 6 th Workshop High Energy Density High Power RF. Ser. AIP Conf. Proc., 2003, vol. 691, p22.
- [8] R. Pakter and C. Chen, *Phys. Rev. E* **62**, 2789 (2000).
- [9] J. Zhou, R. Bhatt and C. Chen, submitted to *Phys. Rev. Lett* (2005).
- [10] R. Bhatt and C. Chen, *Phys. Rev. ST-AB* **8**, 014201 (2005).